Heterogeneous Reaction HOCl + HBr → BrCl + H_2O on Ice Films

Liang Chu and Liang T. Chu*

Department of Environmental Health and Toxicology, State University of New York at Albany and Wadsworth Center, P.O. Box 509, Albany, New York 12201-0509

Received: August 18, 1998; In Final Form: November 23, 1998

The heterogeneous reaction HOCl + HBr(s) → BrCl + H_2O(s) on the ice surface at 189 and 220 K has been investigated in a flow reactor interfaced with a differentially pumped quadrupole mass spectrometer. Pseudo first-order decay of HOCl over the HBr-treated ice surfaces has been determined under the condition of $P_{HOCl} < P_{HBr}$. For the HBr partial pressure in the range of 1.1×10^{-7} to 6.6×10^{-5} Torr, the reaction probability (γ_g) was determined in the range of 0.06 to 0.38 at 189 K. The reaction probability is in the range of 0.01 to 0.07 at 220 K for HBr partial pressure from 7.2×10^{-7} to 1.3×10^{-5} Torr. The reaction probability was found to be strongly dependent on the ice surface temperature. The reaction probability is higher at the lower temperature than that at the warmer temperature and a mechanistic explanation is provided. The "true" reaction probabilities (γ_t) of the reaction were calculated using a pore diffusion model. The kinetic analysis indicates that the heterogeneous reaction of HOCl + HBr may follow the Eley−Rideal type of mechanism. Also, the heat of uptake of HOCl on ice was determined to be about -8.5 ± 2 kcal/mol.

I. Introduction

Heterogeneous reactions on the surface of polar stratospheric clouds (PSCs) are critical to an understanding of the annual appearance of the Antarctic ozone hole. The key chemical processes that occur on polar stratospheric cloud particles responsible for ozone depletion are heterogeneous chlorine reactions 1−2:[1,2]

$$ClONO_2(g) + HCl(s) \rightarrow Cl_2(g) + HNO_3(s) \quad (1)$$

$$HOCl(g) + HCl(s) \rightarrow Cl_2(g) + H_2O(s) \quad (2)$$

The atmospheric chemistry of bromine species is characterized by their short lifetimes and their ready availability for gas-phase catalytic cycles. Even though bromine species have a low concentration in the lower stratosphere, heterogeneous bromine reactions are still important to rapidly convert bromine reservoir compounds $BrONO_2$ and HBr into photochemically reactive species. This process is especially important when it is coupled with the reservoir chlorine species. The following heterogeneous reactions 3 and 4 that involve both bromine and chlorine are of interest to study:[3,4]

$$HOCl(g) + HBr(s) \rightarrow BrCl + H_2O(s) \quad (3)$$

$$HOBr(g) + HCl(s) \rightarrow BrCl + H_2O(s) \quad (4)$$

The significance of these reactions is reflected in several aspects. The heterogeneous reactions can proceed in the dark winter of the polar region and convert photochemically inactive chlorine and bromine reservoir compounds into photochemically reactive species such as Cl_2 or BrCl. When spring comes and light becomes available, Cl_2 or BrCl is photolyzed to produce Cl or Br radicals which then subsequently deplete polar ozone through catalytic cycles.[5,6]

It is worth mentioning that atmospheric bromine species are responsible for about 25% of polar ozone depletion and that ozone destruction efficiency by bromine on a per atom basis is about 50 times more than that of chlorine in the lower stratosphere.[2]

Characterizing the interaction of HOCl, HBr, and HCl with ice is the first step toward revealing the reaction mechanism of reactions 2 and 3. While the uptake of HCl[7−14] and HOCl on ice[13,15−17] were reported in the literature by several groups, the uptake of HBr on ice films at the polar stratospheric temperature was limited to a few studies.[3,18,19] It appears that the uptake of HBr on ice surfaces is higher than that of HCl in general. The higher uptake amount was explained by the formation of solid hydrobromic acid hydrates during the uptake process.[18] Another possible explanation for the higher uptake is that a phase other than HBr-in-ice solid solution is likely to have occurred in the experiments.[19]

While HBr tends to form a hydrate, which is an ionic crystal, near the ice surface at $\sim 10^{-7}$ Torr and 188 K,[18,20] HCl is dissociatively adsorbed on the ice surface.[21] This difference may alter the reaction HOCl + HBr → BrCl + H_2O. It may behave differently from the reaction HOCl + HCl → Cl_2 + H_2O. The heterogeneous reaction HOCl + HCl → Cl_2 + H_2O on ice surfaces has been investigated by a few groups,[13,15,17,22] and HOBr + HCl → BrCl + H_2O on ice has been studied by Abbatt[3] and Allanic et al.[23] Abbatt also studied the heterogeneous reactions HOBr + HBr → Br_2 + H_2O on ice.[3] To the best of our knowledge, there is no reported study for the reaction HOCl + HBr → BrCl + H_2O on ice at stratospheric temperature. With the importance of understanding polar ozone depletion and revealing the nature of chlorine and bromine species interacting with the ice surface, we were motivated to study the heterogeneous reaction HOCl + HBr → BrCl + H_2O and compare this reaction to the HOCl + HCl → Cl_2 + H_2O reaction.

In this paper, we report the first measurement of reaction probability for the reaction HOCl + HBr → BrCl + H_2O on ice surfaces at 189 and 220 K. In the following sections, we

* Author to whom correspondence should be addressed. E-mail: lchu@cnsvax.albany.edu.

10.1021/jp983407n CCC: $18.00
Published on Web 01/22/1999

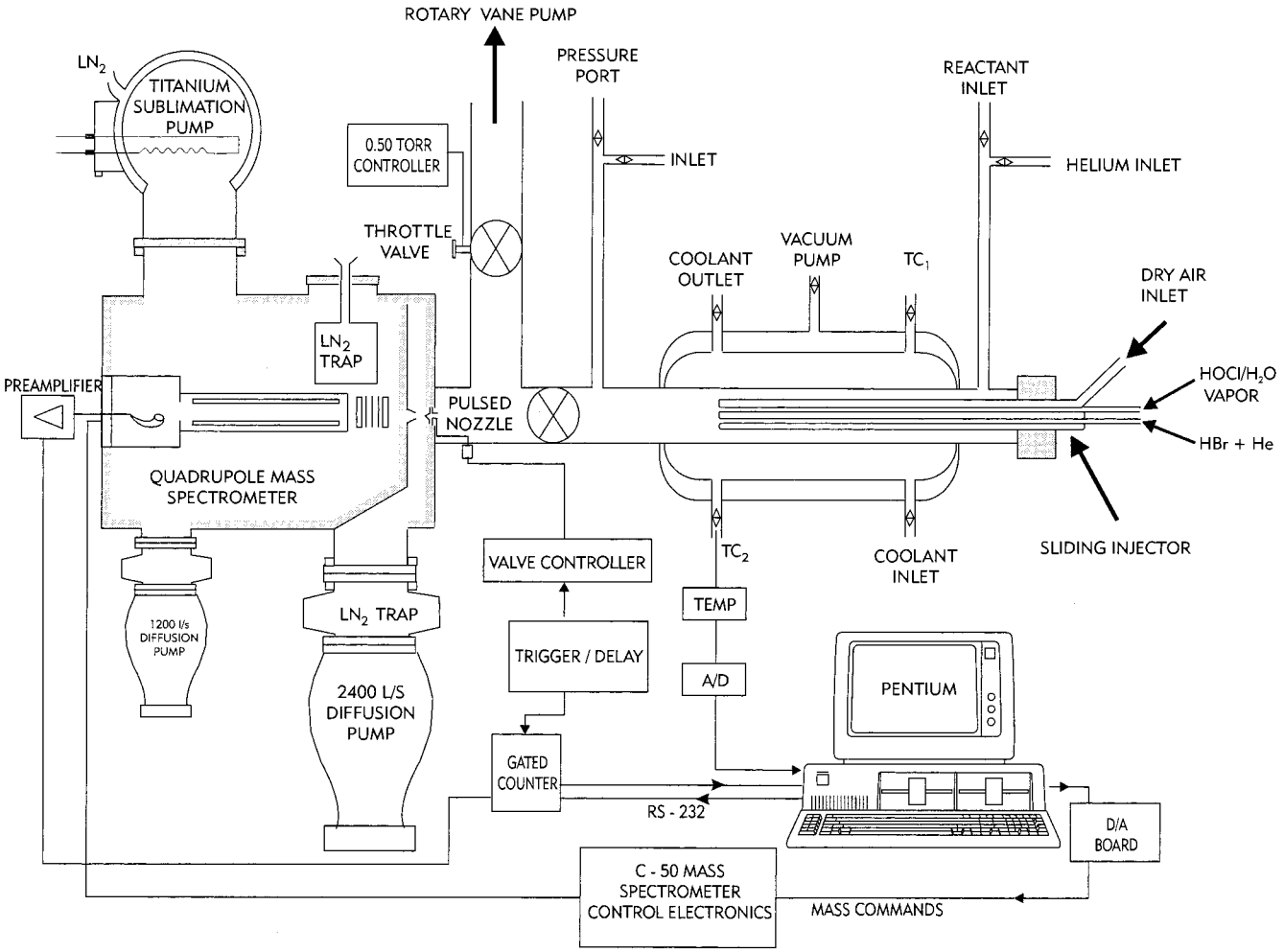

Figure 1. Schematic diagram of the experimental apparatus. The sliding injector with double capillary inlets was used to deposit water-ice on the wall of the flow reactor and to admit HOCl, HCl, and HBr into the reactor. A QMS was employed to monitor HOCl, HCl, HBr, and BrCl concentrations before, during, and after the reaction.

will briefly describe the experimental procedures used in reaction probability measurements and present the experimental results. These include the reaction probability as a function of partial HBr pressures and ice film surface temperatures. We will briefly discuss the reaction mechanism and the effect of temperature on the reaction probability. Finally, we compare the results of reaction 3 and reaction 2.

II. Experimental Section

The reaction probability measurements were performed in a flow reactor coupled to a differentially pumped quadrupole mass spectrometer (QMS). The experimental apparatus is shown in Figure 1. A part of the apparatus has been discussed in our previous publications,[18,24] and we provide only a brief description and some modifications in this paper.

Flow Reactor. The cylindrical flow reactor was constructed of Pyrex glass. Its dimensions were 1.70 cm inner diameter and 35 cm length. The temperature of the reactor was regulated by a liquid-nitrogen-cooled methanol circulator and was measured with a pair of J-type thermocouples located in the middle and at the downstream end. During the experiment, the temperature was maintained at either 189 or 220 K and the stability of the temperature was better than 0.3 K in every experiment. The pressure inside the reactor was controlled by a downstream throttle valve (MKS Instrument, Model 651C), and the stability of the pressure was better than 0.001 Torr in every experiment. A double capillary injector was used to admit both HOCl and HBr into the flow reactor during the reaction probability measurement. Reactant HOCl vapor was taken from the HOCl solution. HOCl vapor contained a small amount of water vapor. To avoid water vapor condensing on the capillary wall at low temperature, dry air was passed through the outside of the capillary.

Ice-Film Preparation. The ice film was prepared as follows: helium carrier gas was bubbled through a constant-temperature 293.2 ± 0.1 K water reservoir. Helium saturated with water vapor was admitted to an inlet of the sliding Pyrex injector. During the course of ice deposition, the sliding injector was slowly pulled out at a constant speed and a uniform ice film was deposited on the inner surface of the reactor, which was at either 189 or 220 K. The amount of ice substrate deposited was determined from the mass flow rate of the water vapor and the deposition time. In a typical experiment at 189 K, the mass of the ice substrate deposited on the flow reactor wall was about 30 mg. An average film thickness was calculated by using the measured ice-film geometric area, the mass of ice, and the bulk density, 0.63 g/cm^3, of vapor-deposited water ice.[25] The typical average film thickness is 2.4 ± 0.2 μm at 189 K and 42 ± 4 μm at 220 K. Note the ice film deposited at 220 K was considerably thicker than the ice film deposited at 189 K. At 220 K, the ice film sublimation rate was higher than that at 189 K.[26] The loss of the ice film due to the evacuation in the

flow reactor would also be larger. Along with the higher total pressure, we had to prepare a thicker film so that the film loss was minimum when the ice was treated by HBr. During the reaction, additional water vapor from the HOCl solution could compensate for the loss of ice.

HBr−He and HCl−He Mixtures. The HBr−He mixture was prepared by mixing HBr (Matheson, 99.8%) and helium (MG, Scientific grade 99.9995%) in an all-glass manifold, which had been previously evacuated to 2×10^{-6} Torr. The typical HBr-to-He mixing ratio is 10^{-3} to 10^{-5}. HBr along with additional helium carrier gas was introduced into the flow reactor via the glass and Teflon PFA tubing, and the amount was controlled by a stainless steel flow controller (Teledyne-Hastings). The HCl−He mixture was prepared by a similar method. The typical mixing ratio was nearly identical to the HBr-to-He ratio.

HOCl Preparation and Calibration. The HOCl solution was prepared by mixing an NaOCl solution with a $MgSO_4$ solution.[27] Forty grams of $MgSO_4 \cdot 7H_2O$ was dissolved in 75 mL of distilled water. The $MgSO_4$ solution was then added to 75 mL of NaOCl solution (6% active chlorine, Aldrich), drop by drop in the dark. A white precipitate of $Mg(OH)_2$ was formed during the reaction. After completing the synthesis, the $Mg(OH)_2$ precipitate was separated from the solution by decantation. A slightly yellowish, clear HOCl(OCl^-) solution was obtained.

The concentration ratio of HOCl to OCl^- can be changed by the acidity of the solution. Thus, it was important to control the pH of the HOCl solution to achieve a higher HOCl yield. In this study, the HOCl solution was monitored by a UV−visible spectrometer (Beckman DU640). The relative absorption intensity at 230 nm (HOCl) and 290 nm (OCl^-) is an indication of the HOCl concentration in the solution.[28] The absorption intensity at 230 nm was determined as a function of the pH in the solution. We found that the most suitable pH value to produce a higher concentration of HOCl was ∼6.5. However, at a slightly higher pH, ∼7.5, gas-phase Cl_2 can be reduced significantly with the trade-off a lower HOCl yield.

Helium gas was bubbled through the HOCl solution that was maintained at 273.15 K. Both HOCl vapor and a small amount of water vapor from the HOCl solution were admitted into the reactor. The water vapor was used to prevent HOCl decomposition by the reaction of $2HOCl \rightarrow Cl_2O + H_2O$ during the transportation of HOCl into the flow reactor. The water vapor pressure was always controlled to be about equal to the ice vapor pressure at the ice-film temperature.

In the calibration experiment, the concentration of gas-phase HOCl was determined by measuring the product Cl_2 in reaction 2 with HCl in excess at 188 K. We assumed that (1) a 1:1 stoichiometric ratio for the formation of Cl_2 from HOCl was valid in the flow reactor, and (2) all Cl_2 formed was released to the gas-phase and quantitatively measured by the QMS. The concentration of Cl_2 was calibrated by using a pure Cl_2 gas (Praxair, 99.5%) diluted in helium. The relative ionization cross sections for HOCl-to-Cl_2 and HOCl-to-HCl were then determined at different HCl and Cl_2 pressures under the various QMS operating conditions. We also determined the QMS output signal as a function of the HOCl partial pressure and QMS operational conditions. The uncertainty of HOCl concentration was estimated to be in the range of 15−20%.

Determination of the Reaction Probability. The reaction probability of HOCl with HBr on the ice film was determined as follows. First, an ice film was vapor-deposited on the inner wall of the flow reactor. Second, the film surface was treated with HBr at pressures between 1.1×10^{-7} and 6.6×10^{-5} Torr for a period of 10−15 min. The ice surface was not completely saturated by HBr yet, but the concentration of HBr was higher than that of HOCl. If we completely saturated the film, the HBr hydrates would desorb from the surface and the entire film would be evaporated.[18] Finally, HOCl was admitted to the reactor with continuing HBr flow in a separated capillary. The gas-phase loss of HOCl was measured by the QMS at $m/e = 52$ as a function of the injector distance. For a pseudo first-order reaction under the plug-flow condition, the following equation holds for the reactant HOCl:

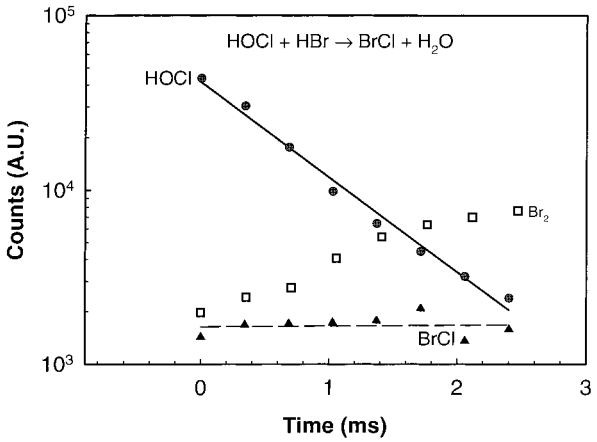

Figure 2. Plot of the HOCl signal versus the reaction time at 189 K. The pseudo first-order rate constant $k_s = 1.25 \times 10^3$ s^{-1} and the corrected rate constant $k_g = 2.08 \times 10^3$ s^{-1}. The reaction probability $\gamma_g = 0.12$. The total pressure = 0.281 Torr and the flow velocity = 29.1 m/s. A signal for product BrCl is also shown in the figure. In a separate experiment, the formation of Br_2 was observed after a short time delay (see text for details).

$$\ln[\mathrm{HOCl}]_t = -k_s(z/v) + \ln[\mathrm{HOCl}]_0 \qquad (5)$$

where z is the injector position, v is the flow velocity, $[HOCl]_t$ is the gas-phase HOCl concentration measured by the QMS at position z, and sub-0 is the initial reference injector position. The injector was typically pulled out 1 cm at a time. The first-order HOCl decay for a typical experiment performed on the ice film at 189 K is shown in Figure 2. The pseudo first-order reaction rate constant, k_s, was calculated from the least-squares fit of eq 5 to the experimental data. k_s was corrected for the gas-phase axial and radial diffusion using a standard procedure,[29] and the corrected rate constant is called k_g. A diffusion coefficient for HOCl in He of 240 Torr·cm^2 s^{-1} at 202 K was used in the calculation.[15] The reaction probability γ_g was calculated from k_g using the following equation:[22]

$$\gamma_g = 2Rk_g/(\omega + Rk_g) \qquad (6)$$

where R is the radius of the flow reactor, and ω is the mean HOCl molecular velocity at the ice-film temperature. In addition, pore diffusion corrections can be made for the reaction probability γ_g and to provide the "true" reaction probability γ_t.[30,31]

III. Results

Uptake of HOCl on Water-Ice. Figure 3 is a plot of the HOCl signal versus the experimental time for the exposure of HOCl on an ice surface. In this experiment, a 28 cm length of the ice film was deposited on the wall of the flow reactor. The gas-phase HOCl signal, as monitored by the QMS at $m/e = 52$, rapidly decreased when HOCl reached the ice surface. Within 2 min, the *entire* ice film was saturated. The uptake amount

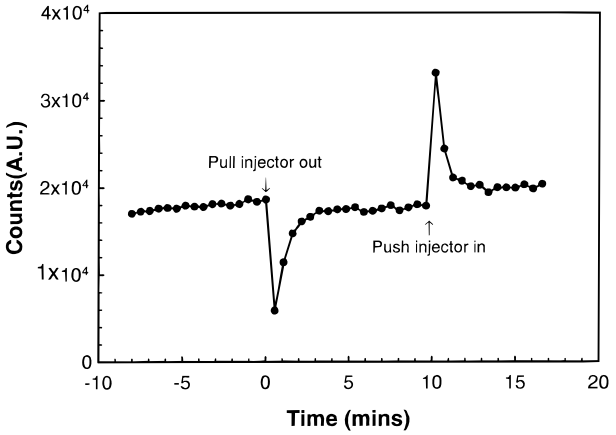

Figure 3. Uptake of HOCl on water-ice at $P_{HOCl} = 1.0 \times 10^{-7}$ Torr and 189 K. (●) represents the HOCl signal. The uptake starts at $t = 0$ min when the injector is pulled out. The entire ice film (150 cm^2) is saturated about 2 min. Desorption occurs at 10 min when the injector is pushed in. This procedure can be repeated several times.

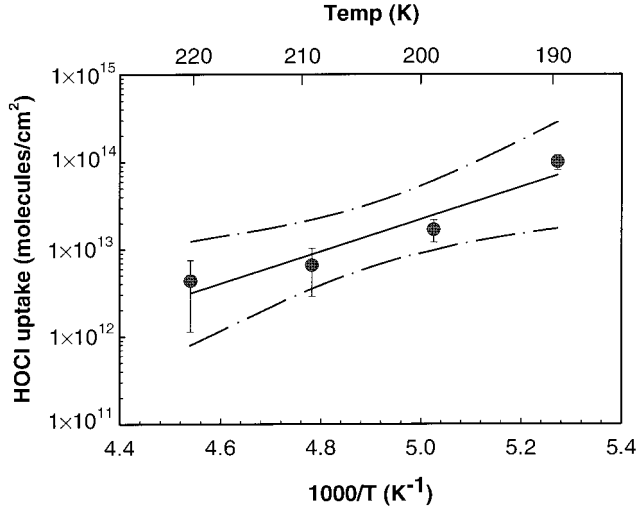

Figure 4. Plot of the logarithm of HOCl surface density versus 1/*T*. The solid line is the least-squares fit to the experimental data, and the dashed lines represent the 95% confidence level. The total pressure was 0.50 Torr, and $P_{HOCl} = 6.0 \times 10^{-7}$ Torr. The "heat of uptake" of HOCl on ice was -8.5 ± 2 kcal/mol.

was determined to be approximately 1×10^{14} molecules/cm^2 at 189 K. When the HOCl-saturated ice film was heated by the injector, HOCl was desorbed and quantitatively recovered as recorded by the QMS. The uptake and desorption procedure could be repeated several times. The uptake amount Θ of HOCl was almost identical to the desorbed HOCl amount. The uptake and desorption process of HOCl on the ice film seems reversible. The uptake of HOCl on the ice film was also measured at different surface temperatures, and the result is shown in Figure 4. The "heat of uptake" of HOCl on ice was calculated from the slope of a plot of log Θ versus 1/*T*. The heat of uptake of HOCl on ice was determined to be -8.5 ± 2 kcal/mol. This is in good agreement with the value of -8.8 kcal/mol and -10.5 kcal/mol by quantum chemistry calculations[16,32] as well as the experimental values of -10.5 ± 2 kcal/mol and -14 ± 2 kcal/mol.[13,15]

HOCl + HBr → BrCl + H_2O. The reaction probability for the HOCl + HBr → BrCl + H_2O reaction was determined by observing the decay of gas-phase HOCl, monitored by the QMS, as a function of the injection position. The reaction probabilities were measured as a function of P_{HBr} in the range 1.1×10^{-7} to 6.6×10^{-5} Torr. Two slightly different partial HOCl pressures were used in this study. P_{HOCl} is about $(5.4 \pm 1.4) \times 10^{-7}$ Torr when $P_{HBr} \geq 1.1 \times 10^{-6}$ Torr, and P_{HOCl} is $(1.5 \pm 0.7) \times 10^{-7}$ Torr when $P_{HBr} < 1.1 \times 10^{-6}$ Torr. The concentration of HBr was always greater than that of HOCl, thus the pseudo first-order condition was satisfied. The reaction probability γ_g as a function of P_{HBr} at 189 and 220 K is presented in Figure 5. The detailed experimental conditions are listed in Table 1. All data listed in the table were averaged over 3 to 10 measurements. The errors in both Table 1 and Figure 5 represent one standard deviation ($\pm\sigma$) of the average value. Figure 5 indicates that the reaction probability γ_g increased from 0.06 to 0.38 as P_{HBr} increased and became less pressure dependent at $P_{HBr} > 2 \times 10^{-5}$ Torr at 189 K. At a warmer temperature, 220 K, the reaction probability γ_g showed a similar trend, that is, it increased from 0.01 to 0.07 as P_{HBr} increased. However, the reaction probability at 220 K was lower than that at 189 K. The ice-film roughness can also be taken into the consideration by using a layer model to calculate the "true" reaction probability.[30,31] The corrected reaction probability γ_t using a tortuosity factor $\tau = 4$ and true ice density $\rho_t = 0.925$ g/cm^3 is also listed in Table 1. γ_t was approximately a factor of 2−10 smaller than γ_g. At a higher γ_g, the reaction is completed before HOCl reaches an internal ice surface and the correction for γ_t is smaller. At a lower γ_g, the HOCl molecule has a chance to enter an internal surface and so the γ_t correction is larger.

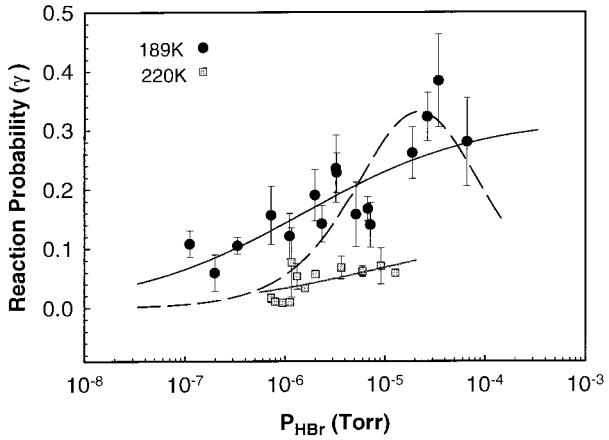

Figure 5. Plot of the reaction probability γ_g versus partial HBr pressures for the reaction of HOCl + HBr on the ice surface at 189 and at 220 K, respectively. Ice film thickness was 2.4 ± 0.2 μm at 189 K and 42 ± 4 μm at 220 K. The error bars represent one standard deviation ($\pm\sigma$) of a mean γ_g value. The solid curves were fitted to the Eley−Rideal mechanism, and the dashed line was fitted to the Langmuir−Hinshelwood mechanism.

A reaction product, BrCl, was measured by the QMS at its parent peak $m/e = 114$. The increase of the BrCl signal was so small that it was hardly detected by the QMS at 189 K (see Figure 2), and in many circumstances the BrCl signal appeared unchanged as the reaction proceeded. This seems to suggest that BrCl was adsorbed on the surface if it was formed during the reaction. We will discuss this in a later section.

We also measured the reaction probability as a function of P_{HOCl} while keeping P_{HBr} as a constant, 3.20×10^{-6} Torr, at 189 K. The result is shown in Figure 6 and Table 2. The experimental data indicate that the reaction probability was nearly independent of the partial HOCl pressure in the range 3.5×10^{-8} to 8.5×10^{-7} Torr.

HOCl + HCl → Cl_2 + H_2O. The reaction probability for the reaction HOCl + HCl → Cl_2 + H_2O was measured in a similar fashion. The thickness of the ice film was 2.5 ± 0.2

TABLE 1: Reaction Probability for the Reaction HOCl + HBr → BrCl + H_2O on Ice Films[a,b]

temperature (K)	P_{HBr} (Torr)	v (m/s)	k_s (1/s)	k_g (1/s)	γ_g	γ_t[c]
188.4 ± 0.1	1.11×10^{-7}	28.7	1.01×10^{3}	1.51×10^{3}	0.09	0.024
188.9 ± 0.6	1.98×10^{-7}	29.1	6.90×10^{2}	8.90×10^{2}	0.06	0.014
188.5 ± 0.1	3.33×10^{-7}	28.7	1.14×10^{3}	1.82×10^{3}	0.11	0.031
188.8 ± 0.1	7.22×10^{-7}	28.8	1.41×10^{3}	2.61×10^{3}	0.16	0.051
188.6 ± 0.2	1.10×10^{-6}	28.9	1.18×10^{3}	1.92×10^{3}	0.12	0.035
189.0 ± 0.1	1.98×10^{-6}	29.0	1.63×10^{3}	3.48×10^{3}	0.19	0.063
189.6 ± 0.1	2.33×10^{-6}	29.4	1.34×10^{3}	2.37×10^{3}	0.14	0.043
189.1 ± 0.6	3.22×10^{-6}	29.4	1.71×10^{3}	3.84×10^{3}	0.24	0.084
189.0 ± 0.4	3.27×10^{-6}	29.1	1.76×10^{3}	4.13×10^{3}	0.23	0.080
188.8 ± 0.1	5.14×10^{-6}	29.1	1.35×10^{3}	2.40×10^{3}	0.16	0.051
188.4 ± 0.3	6.72×10^{-6}	28.8	1.52×10^{3}	3.01×10^{3}	0.17	0.055
188.8 ± 0.2	7.15×10^{-6}	29.0	1.31×10^{3}	2.28×10^{3}	0.14	0.043
188.6 ± 0.1	1.87×10^{-5}	29.0	1.87×10^{3}	4.81×10^{3}	0.26	0.10
188.2 ± 0.2	2.65×10^{-5}	29.1	2.08×10^{3}	6.53×10^{3}	0.32	0.12
188.4 ± 0.2	3.43×10^{-5}	26.1	2.01×10^{3}	7.09×10^{3}	0.38	0.15
188.7 ± 0.1	6.62×10^{-5}	29.4	1.88×10^{3}	4.84×10^{3}	0.27	0.10
220.8 ± 0.7	7.21×10^{-7}	17.9	2.43×10^{2}	2.76×10^{2}	0.016	0.002
219.8 ± 0.5	7.93×10^{-7}	18.3	1.68×10^{2}	1.83×10^{2}	0.011	0.001
220.3 ± 0.3	9.42×10^{-7}	18.2	1.44×10^{2}	1.55×10^{2}	0.009	0.001
220.3 ± 0.2	1.11×10^{-6}	18.4	1.54×10^{2}	1.67×10^{2}	0.010	0.001
219.3 ± 1.2	1.16×10^{-6}	17.8	7.17×10^{2}	1.11×10^{3}	0.063	0.015
220.3 ± 0.8	1.32×10^{-6}	18.8	6.22×10^{2}	8.87×10^{2}	0.051	0.011
220.6 ± 0.5	1.58×10^{-6}	18.1	4.54×10^{2}	5.85×10^{2}	0.034	0.006
220.0 ± 0.5	2.01×10^{-6}	18.2	6.93×10^{2}	1.05×10^{3}	0.060	0.014
221.4 ± 0.1	3.64×10^{-6}	18.5	7.74×10^{2}	1.24×10^{3}	0.070	0.017
220.5 ± 0.1	5.96×10^{-6}	18.6	7.26×10^{2}	1.12×10^{3}	0.064	0.015
221.3 ± 0.1	9.10×10^{-6}	19.3	7.81×10^{2}	1.24×10^{3}	0.070	0.017
219.3 ± 0.1	1.27×10^{-5}	18.8	7.10×10^{2}	1.08×10^{3}	0.062	0.014

[a] All data points are averages of 3 to 10 measurements. [b] Mean total pressure was 0.279 ± 0.008 Torr at 188.7 K and 0.506 ± 0.013 Torr at 220.3 K. Ice film thickness was 2.4 ± 0.2 μm at 188.7 K and 42 ± 4 μm at 220.3 K. [c] $\gamma_t = \dfrac{\sqrt{2}\gamma_g}{\pi\{1+\eta[2(N_L-1)+(3/2)^{1/2}]\}}$ where η is the effectiveness factor as defined in ref 30 and N_L is the number of granule layers. N_L is 5 and 17 for the thin and thick film, respectively.

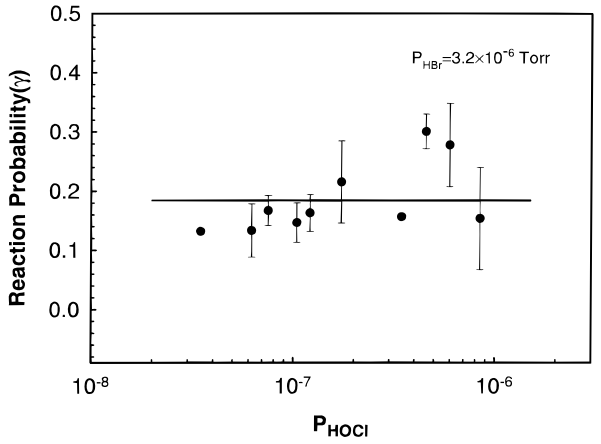

Figure 6. Plot of the reaction probability versus the partial HOCl pressure at 188.5 K. The total pressure in the reactor was 0.278 Torr, and $P_{HBr} = 3.20 \times 10^{-6}$ Torr. The reaction probability γ_g was nearly independent of P_{HOCl}.

μm, and the temperature was 188.4 ± 0.2 K. The reaction probability measured as a function of P_{HCl} at 188 K is presented in Figure 7. Also, both γ_g and γ_t are tabulated in Table 3 along with detailed experimental conditions. For comparison purposes, we choose to use γ_g in all plots, since γ_g is widely used in the atmospheric chemistry literature. Figure 7 indicates that the reaction probability increased slightly at lower HCl pressure, then became less pressure dependent at $P_{HCl} > 1.5 \times 10^{-6}$ Torr.

IV. Discussion

Effect of Temperature on the Reaction HOCl + HBr → BrCl + H_2O. Usually surface reactions are the nonactivated type and the rate constant of a surface reaction does not strongly depend on the temperature.[33] Figure 5 shows that the reaction probability strongly depends on the ice-film surface temperature. This may be attributed to the following two factors. (1) A higher HOCl uptake at 189 K (see Figure 4) indicates that a stronger interaction between HOCl and the ice surface at the lower temperature. The bond strength within a HOCl molecule could be weaker under this circumstance. At a warmer temperature, a weaker interaction between HOCl and ice is less favorable for reaching the transition state and a higher reaction barrier is expected. (2) the desorption of HBr on ice occurs at about 220 K in the fast flow reactor with the total pressure of 0.50 Torr. This is illustrated in Figure 8a. As expected, the peak desorption temperature T_p increases as the heating rate increases. The activation energy for desorption E_a is calculated on the basis of both the peak desorption temperature and the heating rate β by[33]

$$\ln\left(\frac{\beta}{k_B T_p^2}\right) = -\frac{E_a}{k_B T_p} - \ln\left(\frac{E_a}{k_0 \theta_0^{n-1}}\right) \qquad (7)$$

where θ_0 is the coverage at the start of the thermal desorption curve. k_0 is the preexponential factor. k_B is the Boltzmann constant. E_a was determined to be 11.1 ± 3.5 kcal/mol (see Figure 8b). The peak desorption temperature of 220 K implies that the residence time of HBr on the surface decreases dramatically at the desorption temperature and HBr is not readily available for the reaction. Thus, a reduced reaction rate is expected near or above the desorption temperature and the above. It is useful to point that double desorption peaks, separated by ~5 K, were observed in some higher surface coverage experiments. This indicates the formation of a "new" adsorbed species and is consistent with the formation of a hydrate. Likely, HBr desorption is a main reason to explain the

TABLE 2: Reaction Probability for the Reaction HOCl + HBr → BrCl + H_2O on Ice Films[a,b]

temperature (K)	P_{HOCl} (Torr)	thickness (μm)	v (m/s)	k_s (1/s)	k_g (1/s)	γ_g
189.2 ± 0.1	(8.5 ± 0.3) × 10^{-7}	2.4	29.3	1.34 × 10^3	2.78 × 10^3	0.15
189.1 ± 0.1	(6.0 ± 0.2) × 10^{-7}	2.5	29.1	1.85 × 10^3	5.43 × 10^3	0.28
189.1 ± 0.2	(4.6 ± 0.2) × 10^{-7}	2.6	29.1	2.05 × 10^3	5.75 × 10^3	0.30
189.4 ± 0.1	(3.5 ± 0.1) × 10^{-7}	2.4	29.1	1.48 × 10^3	2.76 × 10^3	0.16
188.1 ± 1.1	(1.7 ± 0.2) × 10^{-7}	2.7	28.9	1.66 × 10^3	4.02 × 10^3	0.22
187.8 ± 0.1	(1.2 ± 0.1) × 10^{-7}	2.6	29.2	1.49 × 10^3	2.88 × 10^3	0.16
188.0 ± 0.6	(1.0 ± 0.1) × 10^{-7}	2.5	29.2	1.35 × 10^3	2.61 × 10^3	0.15
188.4 ± 0.1	(7.5 ± 0.1) × 10^{-8}	2.7	29.1	1.51 × 10^3	2.97 × 10^3	0.17
188.4 ± 0.1	(6.2 ± 0.4) × 10^{-8}	2.4	28.6	1.25 × 10^3	2.35 × 10^3	0.13
187.7 ± 0.1	(3.5 ± 0.1) × 10^{-8}	2.5	29.7	1.33 × 10^3	2.28 × 10^3	0.13

[a] Data are mean values. [b] Mean total pressure was 0.278 ± 0.004 Torr. Mean temperature was 188.5 ± 0.6 K. Ice film thickness was 2.5 ± 0.2 μm. P_{HBr} =(3.20 ± 0.30) × 10^{-6} Torr.

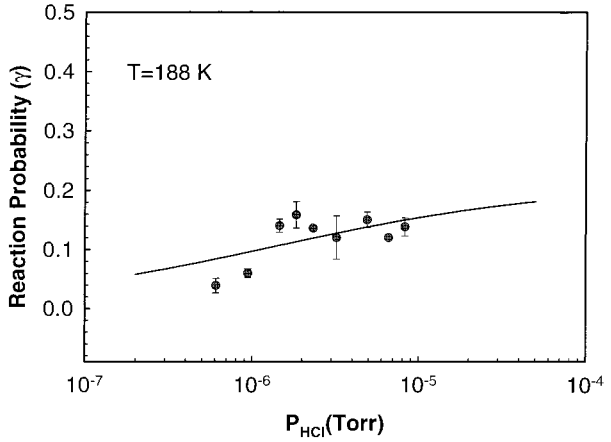

Figure 7. Plot of the reaction probability versus the partial HCl pressure for the reaction of HOCl with HCl on ice at 188 K. The total pressure in the reactor was 0.277 Torr and P_{HOCl} = 7.2 × 10^{-7} Torr. The error bars represent one standard deviation of the mean value. The solid curve was fitted to the Eley−Rideal mechanism. Partial HCl pressure was always larger than partial HOCl pressure.

TABLE 3: Reaction Probability for the Reaction HOCl + HCl → Cl_2 + H_2O on Ice Films at 188 K[a]

temperature (K)	P_{HCl} (Torr)	v (m/s)	k_s (1/s)	k_g (1/s)	γ_g	γ_t
188.5 ± 0.1	6.04 × 10^{-7}	28.4	5.24 × 10^2	6.35 × 10^2	0.04	0.01
188.4 ± 0.1	9.39 × 10^{-7}	28.9	7.58 × 10^2	1.01 × 10^3	0.06	0.01_4
188.5 ± 0.1	1.45 × 10^{-6}	28.5	1.35 × 10^3	2.44 × 10^3	0.14	0.04_3
188.0 ± 0.2	1.83 × 10^{-6}	28.8	1.44 × 10^3	2.74 × 10^3	0.16	0.05_1
188.6 ± 0.1	2.31 × 10^{-6}	28.5	1.33 × 10^3	2.38 × 10^3	0.14	0.04_3
188.3 ± 0.1	3.20 × 10^{-6}	28.2	1.21 × 10^3	2.02 × 10^3	0.12	0.03_5
188.5 ± 0.1	4.90 × 10^{-6}	28.4	1.39 × 10^3	2.58 × 10^3	0.15	0.04_7
188.2 ± 0.1	6.59 × 10^{-6}	28.4	1.19 × 10^3	1.97 × 10^3	0.12	0.03_5
188.6 ± 0.1	8.26 × 10^{-6}	28.6	1.33 × 10^3	2.37 × 10^3	0.14	0.04_3

[a] Total pressure was 0.277 ± 0.006 Torr. Ice film thickness was 2.5 ± 0.2 μm. P_{HOCl} = (7.2 ± 1.2) × 10^{-7} Torr.

temperature dependence of γ_g. These results show that the heterogeneous reaction of HOCl + HBr on ice is largely influenced by temperature in the 189 to 220 K range. This finding may play an important role in understanding the heterogeneous chemistry that occurs near the PSC surface.

Reaction Mechanism. The reaction mechanism is a way to express the nature of the chemical reaction. Two types of surface reactions are commonly found involving two reactants.[33] They are (1) the Langmuir−Hinshelwood mechanism in which both molecules are adsorbed on the surface and then react with each other and (2) the Eley−Rideal mechanism in which one molecule is adsorbed and the other gas-phase molecule reacts with the adsorbed molecule. The chemical reactions occurring near the ice surface at about 190−200 K may not exactly follow these ideal surface reaction types. Either HBr or HOCl molecules

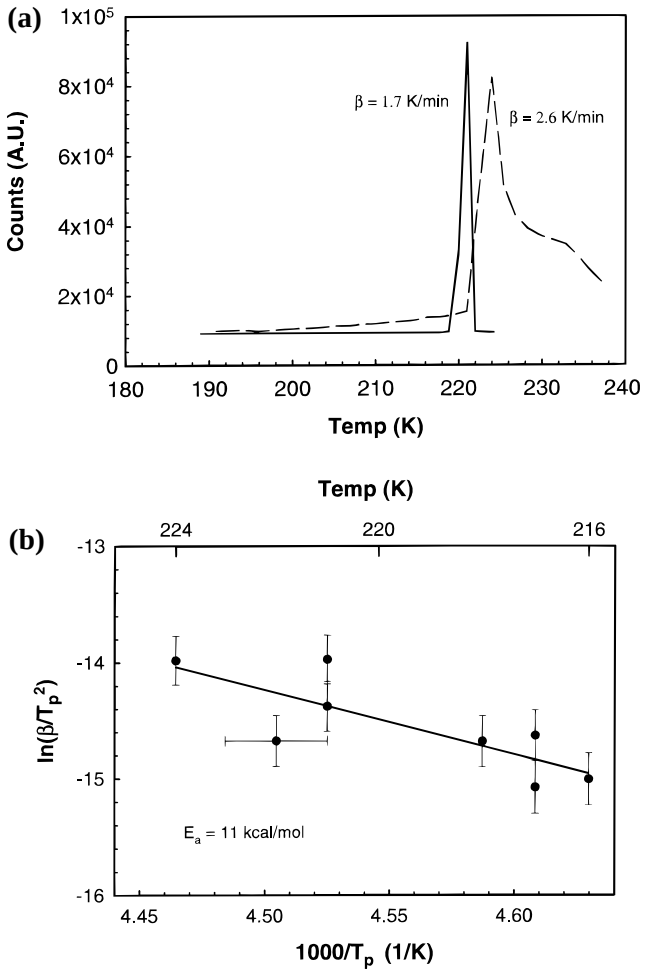

Figure 8. (a) The HBr desorption temperature profile on the ice surface. The solid line indicates a desorption peak temperature T_p of ~221 K with a heating rate β = 1.7 K/min. The dashed line shows T_p ~ 224K with a heating rate β = 2.6 K/min. The ice thickness was about 3 μm, and the total pressure was 0.5 Torr. (b) Plot of $\ln(\beta/T_p^2)$ versus $1/T_p$ to obtain the activation energy for desorption. The error bars represent one standard deviation ($\pm\sigma$) of the measurements. One horizontal error bar represents a typical error of the temperature about ±1 K. All data in the plot have the similar horizontal error bar, which is not shown in the figure for a better viewing purpose.

may diffuse into the ice bulk to a small extent because the diffusion coefficient is on the order of 10^{-12}−10^{-15} cm^2/s. However, it may be convenient to describe the reaction in terms of the ideal surface reaction *empirically*. This kind of mechanism can provide a simple picture as how the HOCl and HBr molecules react with each other to form products.

Both the Eley−Rideal and Langmuir−Hinshelwood mechanisms were being used to test the experimental data for the

reaction HOCl + HBr → BrCl + H_2O. In the case of the Eley−Rideal mechanism, the reactant HBr chemisorbs onto the surface. Adsorbed HBr can then be "solvated" near the surface and reacts with an incoming gas-phase HOCl molecule to form an HOCl−HBr complex. The rearrangement of bonds within the complex then forms the products. This is illustrated by the following reactions:

$$\mathrm{HBr} + \mathrm{S} \underset{k_2}{\overset{k_1}{\rightleftharpoons}} \mathrm{HBr(ad)} \leftrightarrow \mathrm{H^+(H_2O)(ad)} + \mathrm{Br^-(H_2O)(ad)} \quad (8a)$$

$$\mathrm{H^+Br^-(ad)} + \mathrm{HOCl} \rightarrow \mathrm{HOCl\cdots BrH(ad)} \xrightarrow{k_s} \mathrm{BrCl(ad)} + \mathrm{H_2O(ad)} \quad (8b)$$

$$\mathrm{BrCl(ad)} \underset{k_6}{\overset{k_5}{\rightleftharpoons}} \mathrm{BrCl} + \mathrm{S} \quad (8c)$$

Note we expressed HBr in an ionic form, which can either be a dissociative or hydrate form on the surface. We will discuss this intermediate at the end of this section. We expect that reaction 8b is the rate-determining step. The reasons are (1) the sticking probability of HBr on the ice surface at 200 K is higher than 0.12.[34−36] The uptake of HBr is on the order of 10^{15} molecules/cm^2 and HBr is in excess; (2) HOCl is the limiting agent in this study; and (3) BrCl adsorbed on the surface did not affect the measured γ_g's. Both 8a and 8c are unlikely to be the rate-limiting step. The rate of the reaction R is proportional to the HBr surface coverage, θ_{HBr}, and P_{HOCl}:

$$R = -\frac{dP_{HOCl}}{dt} = k_s \theta_{HBr} P_{HOCl} \quad (9)$$

Reaction probability, γ, is given by R/ϕ_{HOCl}, where $\phi_{HOCl} = P_{HOCl}/\sqrt{2\pi m k_B T}$, m is the mass of HOCl. γ can be expressed by eq 10:

$$\gamma = \frac{R}{\phi_{HOCl}} = \frac{c\frac{k_1 k_s}{k_2} P_{HBr}^{1/2} S_0}{1 + \frac{k_1}{k_2} P_{HBr}^{1/2} + \frac{k_6}{k_5} P_{BrCl}} = \gamma_o \frac{b_{HBr} P_{HBr}^{1/2}}{1 + b_{HBr} P_{HBr}^{1/2} + b_{BrCl} P_{BrCl}} \quad (10)$$

where $c = \sqrt{2\pi m k_B T}$, $b_{HBr} = k_1/k_2$, and $b_{BrCl} = k_6/k_5$. In order to express eq 10 as a Langmuir form, we collected all constants together and called γ_o, which is ck_sS_0, where S_0 is the total number of sites on the surface. The experimental results suggest that both HBr and BrCl are adsorbed on the surface. b_{HBr} and b_{BrCl} (adsorption equilibrium constant) are expected to be on a similar order of magnitude. We have $P_{HBr} > P_{HOCl}$ and so $P_{HBr} > P_{BrCl}$. Therefore, $b_{HBr}P_{HBr}^{1/2} \gg b_{BrCl}P_{BrCl}$ when $P_{HBr} < 10^{-5}$ Torr. The term, $b_{BrCl}P_{BrCl}$, can be ignored from eq 10 and eq 10 can be simplified to

$$\gamma = \gamma_0 \theta_{HBr} = \frac{\gamma_0 b_{HBr} P_{HBr}^{1/2}}{1 + b_{HBr} P_{HBr}^{1/2}} \quad (11)$$

where b_{HBr} is constant at a given temperature. γ_o is the reaction probability on an ice surface at its saturation capacity for HBr. The nonlinear least-squares fitting was used to fit the experimental data to eq 11 (Eley−Rideal type), and the result is shown in Figure 5 as the solid line. γ_o was obtained from the fit to be 0.32 and 0.14 at 189 and 220 K, respectively. By the same token, one can use the Langmuir−Hinshelwood mechanism, $R = k_s\theta_{HOCl}\theta_{HBr,}$ to fit the experimental results. The result of that fit is also shown in Figure 5 as the dashed line; however, the fit is not as good as that of the Eley−Rideal type. Equation 11 also explains that the measured reaction probability is independent of the partial HOCl pressure as indicated in Figure 6. It appears that the reaction follows the Eley−Rideal mechanism *experimentally*. In addition, the desorption temperature of HOCl on ice is about 173−175 K[17,37] and the HOCl surface residence time at 189 K is about milliseconds, estimated on the basis of the heat of HOCl uptake. This fact also supports the idea that the reaction resembles the Eley−Rideal type. The fact seems contrary to the HOCl uptake experiment, and this issue will be discussed in a following paragraph.

The Eley−Rideal mechanism can also be used to explain the HOCl + HCl reaction. The solid line in Figure 7 is the fit to eq 11 where $b_{HBr}P_{HBr}^{1/2}$ is replaced by $b_{HCl}P_{HCl}^{1/2}$ (a dissociative isotherm). The curve represents the experimental data well. The mechanism shows that adsorbed HCl is ionized near the ice surface and then reacts with incoming HOCl molecules to form Cl_2.

The kinetic analysis indicates that the HOCl + HBr reaction follows the Eley−Rideal mechanism. This is a steady-state analysis and does not reveal the reaction time scale. From the gas−surface dynamics standpoint, the desorption temperature means that the distribution of desorbed HOCl molecules is centered at about 173−175 K. A very small fraction of HOCl molecules (tails of the distribution) has the probability to adsorb on the surface at 180 Kelvin. When the ice film is porous and has a large surface area, a measurable uptake may be obtained. This is the case for the HOCl uptake experiment where the entire ice film was exposed to HOCl molecules at once (see Figure 3) and the uptake amount is low.

While the HOCl molecule has a finite lifetime (thousands vibrational cycles) on the surface at 189 K, HOCl may hop many times on the surface before it either reacts with HBr or is desorbed from the surface.[38] If this is the case, the HOCl + HBr reaction can be described as a trapping-mediated Langmuir−Hinshelwood type at a molecular level. Because HOCl physically remains on the surface before it desorbs from the surface, the term "trapping-mediated" is used to describe the process. The trapping-mediated process increases the reaction probability dramatically as to the "single collision" Eley−Rideal type. This explains the high reaction probability ($\gamma > 0.1$) very well. The conclusion of this discussion is that the true rate law in terms of actual surface concentration is probably the trapping-mediated Langmuir−Hinshelwood type but the observable rate law is Eley−Rideal.

We want to comment on an intermediate of the reaction. At 189 K or higher, the dynamic nature of the ice surface is expected to "solvate" HBr molecules near the surface or HBr might ionize even as it adsorbs atop the surface.[39] HBr may also form hydrates under our experimental conditions and hydrobromic hydrates are ionic crystal.[20,35,40,41] Either case indicates that HBr is in an ionic form, Br^-, near the ice surface. The reaction between HOCl and HBr is then expected to be ionic in nature. This was reflected in eq 8b. Mechanistically, it is not possible with our current equipment to establish whether the reaction occurs directly between HOCl + Br^- or via the intermediate H_2OCl^+ followed by reaction with Br^- as an analogue to the HOCl + HCl reaction on ice.[42] A general mechanism proposed by Eigen and Kustin is that the reaction

may occur via the following pathway at a higher pH:[43]

$$HOCl + Br^- \rightarrow [HOCl]Br^- \quad (12)$$

$$[HOCl]Br^- + H^+ \rightarrow BrCl + H_2O \quad (13)$$

In this reaction pathway, hydrated Br^- initiates a nucleophilic attack on the Cl end of the HOCl molecule, similar to the hydrolysis of $ClONO_2$.[44] The orientation of the HOCl molecule is with the H-end down the surface.[32] If we assume a hydrate, say $HBr \cdot 3H_2O$, is formed near the ice surface, both $HBr \cdot 3H_2O$ and $HBr \cdot 2H_2O$ have a $H_5O_2^+Br^-$ group,[41] and a six-membered ring intermediate

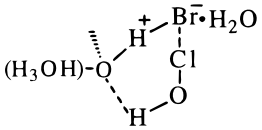

is likely formed. Then a proton transfer follows from a neighboring water molecule to form the products H_2O and BrCl. If the Br-end of BrCl is still bonded to the H_2O surface and the bond is strong, it is possible that BrCl may not desorb to the gas phase. This may be a reason why we did not observe a strong BrCl signal increase in the experiment. Donaldson et al. applied a similar mechanism to the HOCl + HCl reaction in sulfuric acid.[45] Another possible intermediate is a four-centered ring

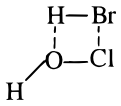

in either hydrated HBr or ionized HBr. Richardson et al. showed that the four-centered intermediate is energetically favorable in the HOCl + HCl reaction with the assistance of Cl^-.[46] It involves a minimum amount of bond breaking and formation. A similar situation may apply to the HOCl + HBr reaction. Both pathways can explain the formation of BrCl. Further experimental and theoretical studies are required to fully resolve the reaction mechanism.

Comparison of the Reaction HOCl + HBr → BrCl + H_2O to HOCl + HCl → Cl_2 + H_2O. The reaction probability for the reaction HOCl + HBr → BrCl + H_2O (eq 3) at 189 K is in the range 0.06−0.38. The reaction probability for the reaction HOCl + HCl → Cl_2 + H_2O (eq 2) at 188 K is in the range 0.04−0.16. The slightly higher reaction probability γ_g for reaction 3 can be explained in terms of the nucleophilicity of the reagent Br^-. Since reactions 2 and 3 are in an identical ice environment, the more nucleophilic reagent has the higher reaction probability. Cl^- is a hard Lewis base; Br^- is a softer Lewis base and thus a better nucleophile to donate its unshared electron pair to HOCl. This results in a higher nucleophilic constant and higher reaction rate.[47] This picture is also consistent with the six-membered ring intermediate as discussed in the previous paragraph.

For reaction 2, the product Cl_2 is always detected in our study. Unlike reaction 2, the gas-phase product BrCl in reaction 3 is produced in small amounts such that the BrCl signal change is nearly undetectable by QMS (see Figure 2). A possible reason is that the product may further proceed through the following heterogeneous sequence in excess HBr:

$$BrCl(s) + HBr(s) \rightarrow Br_2 + HCl(s) \quad (14)$$

Reaction 14 is consistent with our previous discussion that BrCl may adsorb on the ice surface. If reaction 14 is faster than reaction 8c, BrCl will then be converted into Br_2.[19] We examined the product Br_2 at $m/e = 158$. We indeed observed Br_2 formation after a short time delay during the experiment (see Figure 2); however, the amount of Br_2 formed is below the stoichiometric ratio by a factor of 3−5. Hanson and Ravishankara observed a similar phenomenon for the $ClONO_2$ + HBr reaction on ice.[19]

Comparison to Previous Results. For the reaction HOCl + HCl → Cl_2 + H_2O, we may compare our study to previous measurements. Abbatt and Molina reported that the reaction probability γ_g is 0.16 ± 0.10 at 202 K and 0.24 at 195 K.[15] Hanson and Ravishankara measured $\gamma_g > 0.3$ at 200 K.[13] Chu et al. determined the reaction probability is about 0.3 at 188 K.[22] Oppliger et al. reported γ_g is 0.15 at 200 K.[17] Our result is 0.14 at $P_{HCl} = 4.9 \times 10^{-6}$ Torr, $P_{HOCl} = 7.2 \times 10^{-7}$ Torr, and 189 K (see Figure 7). Within uncertainties of measurement, this study is in good agreement with the earlier studies.

For the reaction HOCl + HBr → BrCl + H_2O, Abbatt and Nowak reported that the uptake coefficient is from 0.02 to 0.24 for $P_{HBr} = 1.5 \times 10^{-6} - 7.3 \times 10^{-5}$ Torr in 69.3 wt % sulfuric acid solution at 228 K.[48] We obtained a reaction probability $\gamma_g = 0.06-0.38$ on the ice surface for $P_{HBr} = 1.1 \times 10^{-7} - 6.6 \times 10^{-5}$ Torr at 189 K. The uptake coefficients are comparable for both systems, and the reactive uptake efficiency is very high. Provided the relatively low photolysis rates of HBr ($j = 4.9 \times 10^{-6}$ 1/s)[49] and HOCl ($j = 3 \times 10^{-4}$ 1/s)[50] in the lower stratosphere, this implies that reaction 3 is efficient to convert reservoir Br and Cl, into photochemically active BrCl both on the PSC surface in the dark winter of the polar region and in sulfuric acid aerosols. However, this reaction rapidly consumes all available HBr (~2pptv or less)[2] in a day or so. By then, the reaction is insignificant. The reaction is a source to maintain low concentration of HBr in the polar region.[4] Overall, reaction 3 changes the partitioning of both Br and Cl species and may play a role in bromine heterogeneous chemistry in the lower stratosphere.

V. Conclusion

HOCl saturates the water-ice surface rapidly, and the uptake of HOCl with water-ice is likely a reversible process. The reaction probability γ_g for the HOCl + HBr → BrCl + H_2O reaction ranges from 0.06 to 0.38 at 189 K and from 0.01 to 0.07 at 220 K. The experimental results suggest that the observed rate law for the heterogeneous reaction of HOCl + HBr is the Eley−Rideal type. The results obtained from this study can be extrapolated to stratospheric conditions and can be used in atmospheric chemistry modeling.

Acknowledgment. The authors thank two anonymous reviewers for helpful suggestions and comments on the manuscript. This work was supported by the National Science Foundation under grant ATM-953065.

References and Notes

(1) Solomon, S.; Garcia. R. R.; Rowland, F. S.; Wuebbles, D. J. *Nature* **1986**, *321*, 755.

(2) WMO. *Scientific Assessment of Ozone Depletion: 1994*, Report 37; WMO: Geneva, 1995**;** Chapters 3, 10.

(3) Abbatt, J. P. D. *Geophys. Res. Lett.* **1994**, *21*, 665.

(4) Lary, D. J.; Chipperfield, M. P.; Toumi, R.; Lenton, T. *J. Geophys. Res.* **1996**, *101*, 1489.

(5) Molina, L. T.; Molina, M. J. *J. Phys. Chem.* **1987**, *91*, 433.

(6) McElroy, M. B.; Salawitch, R. J.; Wofsy, S. C.; Logan, J. A. *Nature* **1986,** *321*, 759.

(7) Abbatt, J. P. D.; Beyer, K. D.; Fucaloro, A. F.; McMahon, J. R.; Wooldridge, J. R.; Zhang, R.; Molina, M. J. *J. Geophys. Res.* **1992**, *97*, 15819.
(8) Wofsy, S. C.; Molina, M. J. *J. Geophys. Res.* **1988**, *93*, 2442.
(9) Hanson, D. R.; Mauersberger, K. *J. Phys. Chem.* **1992**, *96*, 7079.
(10) Kroes, G.-J.; Clary, D. C. *J. Phys. Chem.* **1990**, *94*, 4700.
(11) Koehler, B. G.; McNeill, L. S.; Middlebrook, A. M.; Tolbert, M. A. *J. Geophys. Res.* **1993**, *98*, 10563.
(12) Gertner, B. J.; Hynes, J. T. *Science* **1996**, *271*, 1563.
(13) Hanson, D. R.; Ravishankara, A. R. *J. Phys. Chem.* **1992**, *96*, 2682.
(14) Chu, L. T.; Leu, M.-T.; Keyser, L. F. *J. Phys. Chem.* **1993**, *97*, 7779.
(15) Abbatt, J. P. D.; Molina, M. J. *Geophys. Res. Lett*. **1992**, *19*, 461.
(16) Geiger, F. M.; Hicks, J. M.; Dios, A. C. *J. Phys. Chem.* **1998**, *102*, 1514.
(17) Oppliger, R.; Allanic, A.; Rossi, M. J. *J. Phys. Chem. A* **1997**, *101*, 1903.
(18) Chu, L. T.; Heron, J. W. *Geophys. Res. Lett*. **1995**, *22*, 3211.
(19) Hanson, D. R.; Ravishankara, A. R. *J. Phys. Chem.* **1992**, *96*, 9441.
(20) Chu, L. T.; Chu, L. *J. Phys. Chem. A* **1999**, *103*, 384.
(21) Horn, A. B.; Chesters, M. A.; McCoustra, M. R. S.; Sodeau, J. R. *J. Chem. Soc., Faraday Trans.* **1992**, *88*, 1077.
(22) Chu, L. T.; Leu, M.-T.; Keyser, L. F. *J. Phys. Chem.* **1993**, *97*, 12798.
(23) Allanic, A.; Oppliger, R.; Rossi, M. J. *J. Geophys. Res.* **1997**, *102*, 23529.
(24) Chu, L. *J. Vac. Sci. Technol. A.* **1997**, *15*, 201.
(25) Keyser, L. F.; Leu, M.-T. *J. Colloid Interface Sci.* **1993**, *155*, 137.
(26) Haynes, D. R.; Tro, N. J.; George, S. M. *J. Phys. Chem*. **1992**, *96*, 8502.
(27) D'Ans, J.; Freund, H. E. *Z. Elektrochem*. **1957**, *61*, 10.
(28) Molina, L. T.; Molina, M. J. *J. Phys. Chem.* **1978**, *82*, 2410.
(29) Brown, R. L. *J. Res. Natl. Bur. Stand. (U.S.)* **1978**, *81*, 1.
(30) Keyser, L. F.; Moore, S. B.; Leu, M.-T. *J. Phys. Chem.* **1991**, *95*, 5496.
(31) Keyser, L. F.; Leu, M.-T.; Moore, S. B. *J. Phys. Chem*. **1993**, *97*, 2800.
(32) Brown, A. R.; Doren, D. J. *J. Phys. Chem. B* **1997**, *101*, 6308.
(33) Masel, R. I. *Principles of Adsorption and Reaction on Solid Surfaces*, Wiley: New York, 1996; Chapter 7.
(34) Breil, M.; Behr, P.; Zellner, R. *PSI-Proc.* **1997**, *97*−*02*, 35. (γ_{HBr} = 0.12, abstract is available on the CA online.)
(35) Rieley, H.; Aslin, H. D. *J. Chem. Soc., Faraday Trans*. **1995**, *91*, 2349.
(36) Hanson, D. R.; Ravishankara, A. R. in *The Tropospheric Chemistry of Ozone in the Polar Regions*, NATO ASI Series, Niki, H.; Becker, K. H., Eds.; Springer-Verlag: New York , 1993;, pp 281−290.
(37) Bahnam, S. F.; Horn, A. B.; Koch, T. G.; Sodeau, J. R. *Faraday Discuss*. **1995**, *100*, 321.
(38) Weinberg, W. H. in *Dynamics of Gas*−*Surface Interactions* Rettner, C. T., Ashfold, M. N. R., Eds.; RSC: Cambridge, 1991; Chapter 5.
(39) Bianco, R.; Gertner, B. J.; Hynes, J. T. *Ber. Bunsen-Ges. Phys. Chem*. **1998**, *102*, 518.
(40) Delzeit, L.; Rowland, B.; Devlin, J. P. *J. Phys. Chem*. **1993**, *97*, 10312.
(41) Lundgren, J.-O. *Acta Cryst*. **1970**, *B26*, 1893.
(42) Banham, S. F.; Horn, A. B.; Koch, T. G.; Sodeau, J. R. *Faraday Discuss*. **1995**, *100*, 321.
(43) Eigen, M.; Kustin, K. *J. Am. Chem. Soc*. **1962**, *84*, 1335.
(44) Bianco, R.; Hynes, J. T. *J. Phys. Chem*. **1998**, *102*, 309.
(45) Donaldson, D. J.; Ravishankara, A. R.; Hanson, D. R. *J. Phys. Chem.* **1997**, *101*, 4717.
(46) Richardson, S. L.; Francisco, J. S.; Mebel, M. A.; Morokuma, K. *Chem. Phys. Lett.* **1997**, *270*, 395.
(47) Lowry, T. H.; Richardson, K. S. *Mechanism and Theory in Organic Chemistry*, 2nd ed.; Harper & Row: New York, 1981; pp 331−339.
(48) Abbatt, J. P. D.; Nowak, J. B. *J. Phys. Chem. A* **1997**, *101*, 2131.
(49) Yung, Y. L.; Pinto, J. P.; Watson, R. T.; Sander, S. P. *J. Atm. Sci.* **1980**, *37*, 339.
(50) DeMore, W. B.; Sander, S. P.; Golden, D. M.; Hampson, R. F.; Kurylo, M. J.; Howard, C. J.; Ravishankara, A. R.; Kolb, C. E.; Molina, M. J. *Chemical Kinetics and Photochemical Data for Use in Stratospheric Modeling*, Evaluation 12; JPL: Pasadena, CA, 1997; pp 265.